NANO LETTERS

2007
Vol. 7, No. 12
3639−3644

High-Throughput Fabrication of Organic Nanowire Devices with Preferential Internal Alignment and Improved Performance

Zhijun Hu,[†,‡] Benoît Muls,[§] Loïk Gence,[‡,||] Dana A. Serban,[‡,||] Johan Hofkens,[⊥] Sorin Melinte,[‡,||] Bernard Nysten,[†,‡] Sophie Demoustier-Champagne,[†,‡] and Alain M. Jonas*[,†,‡]

Unité de Physique et de Chimie des Hauts Polymères (POLY), Research Center in Micro- and Nanoscopic Materials and Electronic Devices, CeRMiN, Université catholique de Louvain, Place Croix du Sud 1, B-1348 Louvain-la-Neuve, Belgium, Unité de Chimie des Matériaux Inorganiques et Organiques (CMAT), Université catholique de Louvain, Place L. Pasteur 1, B-1348 Louvain-la-Neuve, Belgium, Unité des Dispositifs Intégrés et Circuits Electroniques (DICE), Université catholique de Louvain, Place du Levant 3, B-1348 Louvain-la-Neuve, Belgium, and Department of Chemistry, Katholieke Universiteit Leuven, Celestijnenlaan 200F, 3001 Heverlee, Belgium

Received July 31, 2007; Revised Manuscript Received October 9, 2007

ABSTRACT

We demonstrate that arrays of nanowires of conjugated polymers can be easily produced by a simple embossing protocol, compatible with very large scale integration technology. The embossing process is shown to have the supplementary virtue to increase the internal degree of order of the nanowires, significantly enhancing their performance. This is applied to the fabrication of nanowire-based devices consisting of a liquid crystalline light-emitting polymer, of a liquid crystalline semiconducting polymer, and of an amorphous conducting polymer, illustrating the versatility and wide applicability of the method.

Nanowires of conducting and semiconducting materials have been gaining interest owing to their potential use in sensing devices,[1] miniaturized light sources,[2,3] and integrated electronic nanodevices.[4] Although there are several methods to produce, align, and position nanowires of inorganic materials such as silicon or carbon, the development of appropriate methodologies to fabricate and position nanowires of organic materials has been lagging behind. Here, we show how arrays of nanowires of conjugated polymers can be obtained by a fast and inexpensive embossing process compatible with very large scale integration technology, simultaneously involving the preferential alignment of chains perpendicular or parallel to the nanowire axis, resulting in significantly improved optical or electrical performance. This is demonstrated for materials belonging to three different classes of liquid crystalline or amorphous conjugated polymers, giving rise to conducting, semiconducting, or light-emitting organic nanowires on different substrates, including glass and silicon.

The solution processability of conjugated polymers allows one to easily prepare uniform thin films[5] into which a random bi- or tridimensional orientation of polymer chains and/or crystals is usually obtained. However, the optical and electronic properties of conjugated polymers are intrinsically anisotropic because of the delocalization of π-electrons along their backbones[6] and of the interchain electronic-coupling anisotropy.[7] Therefore, to optimize performance it is critical to align the molecular or crystalline components of these materials in specific directions, which was attempted by methods such as self-assembly,[8] application of external forces,[9−11] Langmuir−Blodgett deposition,[12] and blown-bubble transfer.[13] Unfortunately, most of these methods result in limited ordering or need specific substrates and polymer materials. Few of them are compatible with the requirements of very large scale integration technology.

* Corresponding author. E-mail: alain.jonas@uclouvain.be.
[†] Unité de Physique et de Chimie des Hauts Polymères (POLY), Université catholique de Louvain.
[‡] Research Center in Micro- and Nanoscopic Materials and Electronic Devices, CeRMiN, Université catholique de Louvain.
[§] Unité de Chimie des Matériaux Inorganiques et Organiques (CMAT), Université catholique de Louvain.
[||] Unité des Dispositifs Intégrés et Circuits Electroniques (DICE), Université catholique de Louvain.
[⊥] Katholieke Universiteit Leuven.

10.1021/nl071869j CCC: $37.00 © 2007 American Chemical Society
Published on Web 11/13/2007

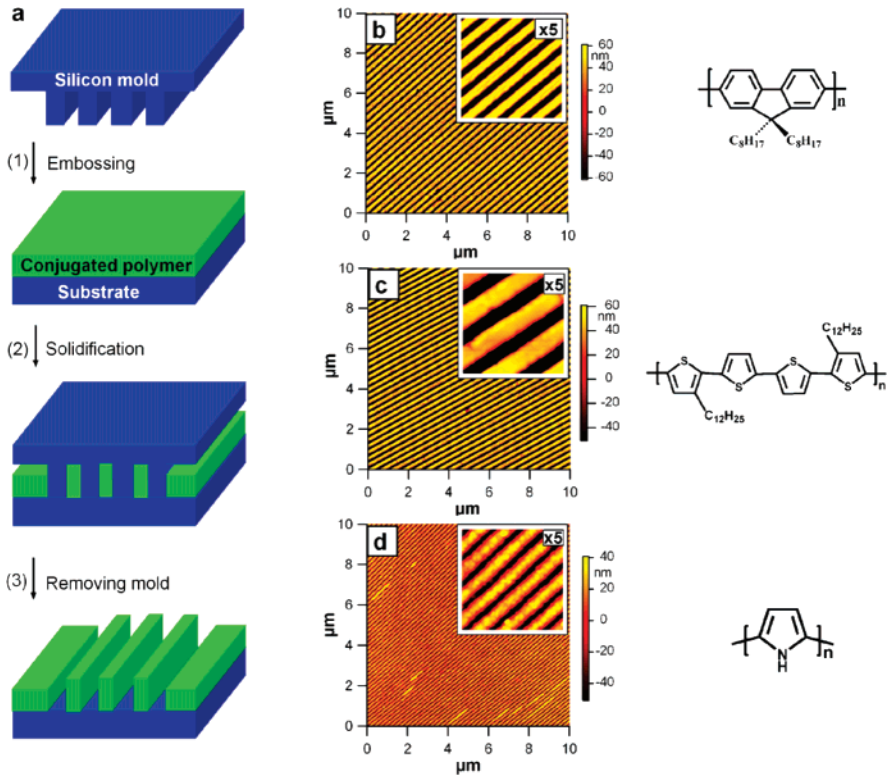

Figure 1. Fabrication of arrays of nanowires of conjugated polymers with internal preferential internal alignment. (a) Schematic outline of the process. (b−d) AFM topography images of nanowire arrays of PFO (b), PQT (c), and PPy (d). The chemical structures of the polymers are shown on the right-hand side.

In addition to the required preferential alignment in two-dimensional architectures, the fabrication of nanowires of (semi)conducting polymers is even more desirable because this would enable the fabrication of miniaturized (opto)-electronic devices or sensors of improved sensitivity, as already demonstrated for inorganic semiconductors. Nanowires of conjugated polymers have been fabricated by lithography[14,15] or templating methods.[16,17] Lithography offers limited resolution or requires elaborate and expensive processing steps and often involves etching techniques that decrease the performance of conjugated polymers.[18] As for templating methods, their development has been thwarted by difficulties in patterning and integrating the produced nanowires.[15] Significantly, few of the reported approaches are capable of controlling the internal order of the nanowires.

Embossing is a rapid and low-cost method allowing to transfer in an initially flat polymer film the topographical features of a mold with the assistance of temperature[19] or solvent vapors.[20] Also known as "nanoimprint lithography",[19] it is used to shape the surface of polymer films for lithographic purposes. Here, we focus on amorphous and liquid crystalline conjugated polymers and use embossing to fabricate arrays of nanowires of improved internal structure with chains preferentially aligned parallel or perpendicular to the nanowire axis, resulting in a significant improvement of performance of devices such as transistors.

The process, shown schematically in Figure 1a, consists of pressing a hard mold bearing nanotrenches into a thin film of a conjugated polymer in a fluid state (a liquid or liquid crystalline phase, or a solvent-swollen plasticized state), followed by the subsequent crystallization of the embossed polymer by cooling or solvent evaporation. The substrate here is a silicon wafer or a glass slide, although it might be any (in)organic material whose surface is planar enough to allow conformal contact with the hard mold. The initial thickness of the film is selected with respect to the depth and period of the nanotrenches defined on the mold to obtain a contact between the protrusions of the mold and the substrate, which results in the formation of parallel isolated nanowires if the interaction between polymer and substrate is sufficiently weak.[21] This is in marked contrast with previous reports on the nanoimprint of films of conjugated polymers that did not produce nanowires but only imprinted features standing out above a continuous film.[22,23] A related technique, "microcutting", was previously used to pattern polymer-supported metal film[24] and to produce vertical-channel polymer field-effect transistors[25] by embossing in the solid state. Although crystallizable polymers were used in these microcutting techniques, a positive effect on the orientation of polymer crystals was not demonstrated because the embossing was performed below the melting point of the semicrystalline polymers.

Examples of atomic force microscopy (AFM) topography images of arrays of nanowires of photo- and electroluminescent poly(9,9-di-*n*-octyl-2,7-fluorene) (PFO), semiconducting poly(3,3‴-didodecyl-quaterthiophene) (PQT), and conducting polypyrrole (PPy) fabricated by the above process are shown in Figure 1b-d. The nanowires are uniform in their heights, widths, and lengths. In the case of PFO and PQT, embossing was performed in the liquid crystalline phase,[26,27]

followed by crystallization upon cooling or annealing (see Supporting Information for experimental details). In both cases, the initial thickness of the films spin-coated on silicon was about 60 nm. The width (from 800 to 80 nm) and length (100 μm) of the nanowires precisely replicates the dimensions of the nanotrenches defined on the print mold, whereas their height is close to the depth of the nanotrenches of the mold (100 nm). The approach is not limited to liquid crystalline conjugated polymers and was applied to PPy, a conducting conjugated polymer of high glass transition temperature usually reported to be amorphous (Figure 1d). In this case, embossing was performed at room temperature, taking advantage of the lowered glass transition of the film resulting from the presence of residual solvent just after spin-coating.

The complete isolation of the nanowires fabricated by our method was confirmed by scanning electron microscopy (Supporting Information) and transmission electron microscopy (TEM) images (Figure 2a,c), which show only faint or even no traces of crystals in the regions between the nanowires. The high degree of preferential orientation of lamellar crystals and/or polymer chains within the nanowires was confirmed by selected area electron diffraction (ED) and polarized optical microscopy (POM). The ED patterns of PFO and PQT nanowires (Figure 2b,d), corresponding to the regions shown in Figure 2a,c, present very well-oriented, single-crystal-like reflections, confirming the high degree of structural order of the chain packing in the nanowires. In the case of PFO, all reflections can be indexed to the (0*kl*) reciprocal lattice section of the α′ form (orthorhombic unit cell with $a = 2.56$ nm, $b = 2.38$ nm, $c = 3.32$ nm).[26] The (00*l*) reflections lie along the long axis direction of the nanowires, showing that the crystallographic *c*-axis, which is parallel to the PFO polymer backbone, is aligned parallel to the long axis of the nanowires. In the case of PQT (Figure 2d), the reflections in the ED patterns can be indexed to the (*hk*0) section (orthorhombic unit cell with $a = 1.72$ nm, $b = 0.37$ nm, $c = 1.21$ nm),[27,28] indicating that the PQT chain backbones are perpendicular to the substrate and to the nanowire axis. The (0*k*0) reflections, which are in the π-stacking direction of PQT, are aligned along the long axis of the nanowires, which should favor high charge mobility along this axis.[7] The transmission electron microscopy (TEM) experiments were performed on PFO nanowires of 80−200 nm width and on PQT nanowires of 90−150 nm width. Similar single-crystal-like ED patterns showing the same general orientation were observed for different locations along nanowires in a given array (over a total length of 100 μm) and also for nanowires of differing widths (from 80 to 200 nm; see Supporting Information), showing how reproducible the method is. We have also obtained TEM images and ED patterns of the nonembossed regions of the samples, where either diffraction spots with different orientations were observed depending on location, or even diffraction rings and arcs when the domain size becomes smaller than the electron beam size (Supporting Information), confirming that the nanoconfined geometry provided by the nanotrenches in the mold is crucial for preferential orientation.

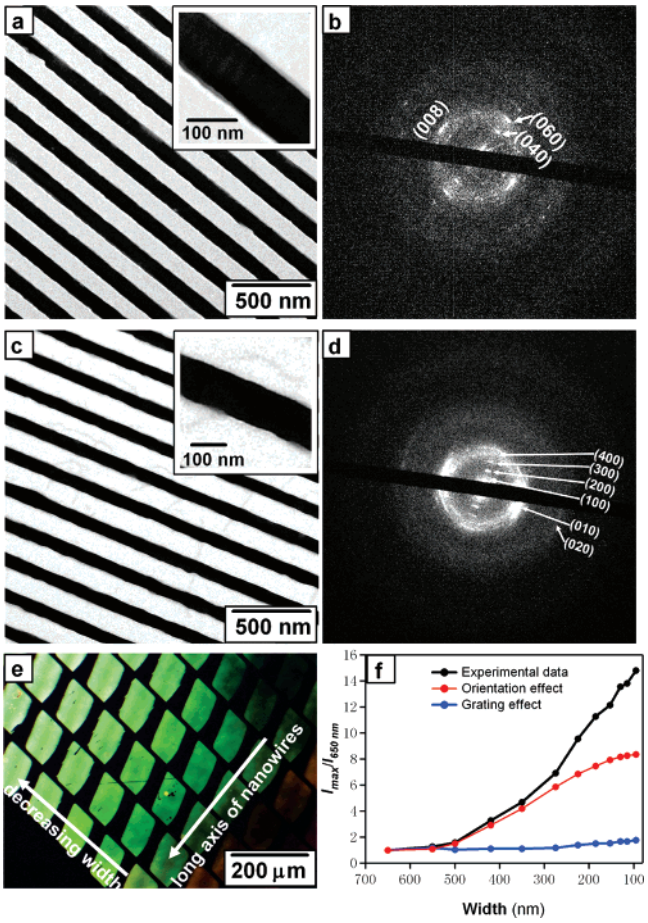

Figure 2. Preferential alignment of crystals and polymer chains within the nanowires. (a,c) TEM image of PFO and PQT nanowires, respectively, showing that no residual polymer layer is left between the (dark) nanowires. (b,d) Corresponding selected area ED pattern of PFO and PQT, respectively, showing preferential crystallographic orientation. For PFO, the chain axis (*c*-axis) is parallel to the nanowire axis. For PQT, the π-stacking direction (*b*-axis) is aligned along the nanowire axis. (e) POM image of PPy nanowires (true colors), with the long axis of nanowires aligned at ∼45° with respect to the crossed-polarizing filters. Every bright region in the image is an array of parallel PPy nanowires, whose widths range from 500 to 130 nm. The birefringence is enhanced for nanowires of smaller width. (f) Ratio of the intensity reflected in POM by arrays of PPy nanowires to the intensity reflected for PPy nanowires of 650 nm width vs the width of the PPy nanowires. We present the experimental data, an upper bound of the reflected intensity arising from subwavelength-grating effects only and the complementary contribution to the birefringence due to the orientation of polymer chains.

The different preferential alignment of PFO and PQT chains, which are respectively parallel and perpendicular to the nanowire axes, can be rationalized by considering the different microscopic structures of their liquid crystalline phases. PQT, which adopts an inverse comblike liquid crystalline phase, forms like many poly(alkyl-thiophene)'s nanometer-sized rodlike structures consisting of extended chains packed with their π-stacking direction along the rod axis.[27] During embossing in the liquid crystalline phase, these rodlike elements align along the grooves; upon cooling, their orientation is preserved, leading to a perpendicular alignment of the chain axis. In contrast, at the embossing temperature

PFO is a nematic liquid crystal whose director is aligned with the chain axis direction. In the liquid crystalline phase, the chains thus align parallel to the groove axis, resulting in a final crystalline morphology where the chain axis is parallel to the groove axis (crystalline lamellae being thus aligned perpendicular to the grooves). This mechanism differs substantially from the one acting for crystalline polymers nanoimprinted in the liquid phase, which were previously shown by us to crystallize grapho-epitaxially in nanogrooves.[29]

Alignment is however not restricted to liquid crystalline systems, as could be demonstrated for the nanowires of amorphous PPy. In this case, TEM images and ED patterns could not be obtained because sample preparation involves floating off the nanostructures on a water solution, which is not compatible with the water solubility of PPy. Therefore, the orientation of PPy nanowires was investigated by POM in reflection. The imprinted samples were positioned between crossed linear-polarizing filters with the long axis direction of nanowires aligned at an angle α with respect to one of the filters. An example of POM image taken at $\alpha \approx 45°$ is shown in Figure 2e. The bright birefringent regions are made of arrays of PPy nanowires of varying width. We present in Figure 2f the ratio between the maximum reflected intensity and the maximum intensity recorded for nanowires of 650 nm width, versus the width of the nanowires. The recorded birefringence may be caused by preferential orientation of the chains in the nanowires and/or result from the fact that the optical properties of a subwavelength grating are equivalent to those of a uniaxial film.[30] An upper bound for the contribution from the grating effect was estimated (Supporting Information) and is shown in Figure 2f, together with the complementary contribution from the internal preferential orientation. The contribution due to the subwavelength grating is minor and of decreasing relative importance with decreasing nanowire width, confirming that preferential orientation of chains is the dominant factor explaining the observed birefringence. In the present case, alignment results from the rigidity of the conjugated chains that upon embossing tend to orient parallel to the groove axis. This indicates that our alignment method is quite general and is not restricted to crystalline or liquid crystalline polymers.

The preferential internal alignment of nanowires fabricated by the embossing method can be attributed to the confinement provided by the vertical walls of the nanogrooves in the mold. As can be seen in Figure 2f, a maximum width of about 400 nm was found to be needed to align the PPy chains. For the liquid crystalline systems such as PFO and PQT, a maximum width of similar order of magnitude was found by optical microscopy to be required to align the polymer chains and/or lamellar crystals, although this value may vary according to the selected crystallization conditions. Further research on the dependence of maximum groove width with respect to crystallization conditions will be performed in the future.

The anisotropic optical properties of the nanowires of PFO, which is an attractive material for light-emitting diodes owing to its efficient blue emission, were assessed by recording

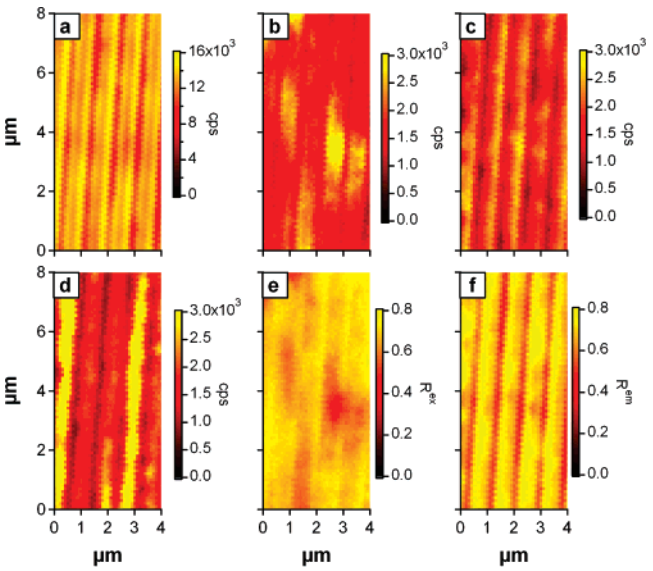

Figure 3. Photoluminescence of PFO nanowires of 650 nm width embossed on cover glass slips. (a,b) Intensity emitted upon excitation by light of linear polarization parallel to the nanowires; the emission is recorded through a polarizing filter set parallel (a) and perpendicular (b) to the nanowire axis. (c,d) Intensity emitted upon excitation by light of linear polarization perpendicular to the nanowires; the emission is recorded through a polarizing filter set parallel (c) and perpendicular (d) to the nanowire axis. Note the difference of color scale between a and b−d. (e) Excitation anisotropy, R^{ex}, computed from (a) and (c). (f) Emission anisotropy, R^{em}, computed from (a) and (b). Both emission and excitation are strongly anisotropic, revealing preferential alignment of the chains, resulting in polarized photoluminescence of the nanowires.

their photoluminescence (PL) with a home-built laser scanning confocal microscope. The nanowires were excited by linearly polarized laser light at $\lambda = 380$ nm with the polarization set parallel to the nanowires, and the PL images were recorded with a polarizing filter (analyzer) set parallel (Figure 3a, $I_{\parallel,\parallel}$) or perpendicular (Figure 3b, $I_{\parallel,\perp}$) to the nanowires. Then, the nanowires were excited with light polarized perpendicular to the nanowires, and the PL images were again recorded with the analyzer parallel (Figure 3d, $I_{\perp,\parallel}$) or perpendicular (Figure 3d, $I_{\perp,\perp}$) to the nanowires. The anisotropy of excitation (Figure 3e, $R^{ex} = (I_{\parallel,\parallel} - I_{\perp,\parallel})/(I_{\parallel,\parallel} + 2I_{\perp,\parallel})$) and of emission (Figure 3f, $R^{em} = (I_{\parallel,\parallel} - I_{\parallel,\perp})/(I_{\parallel,\parallel} + 2I_{\parallel,\perp})$) was then computed from these images. The average anisotropy of excitation is 0.65, whereas it is 0.70 in emission, indicating a high degree of chain alignment and strong polarization of the emitted light.

The electronic properties of PQT nanowires were evaluated within a field-effect transistor (FET) configuration (Supporting Information). Gold source and drain electrodes were deposited on top of the nanowires using TEM grids as shadow masks (Figure 4a). The channel length was 35 μm, whereas the width of the electrodes was $W^{el} = 85$ μm. Drain current (I_{ds}) versus drain-source voltage (V_{ds}) relationships at various gate voltages (V_{bg}) show typical accumulation mode p-channel transistor behavior (Figure 4b), typified by I_{ds} increasing linearly with V_{ds} at low V_{ds} and saturating at higher V_{ds}. The field-effect mobility μ_{lin} was computed from the I_{ds} versus V_{bg} characteristics (displaying a negligible

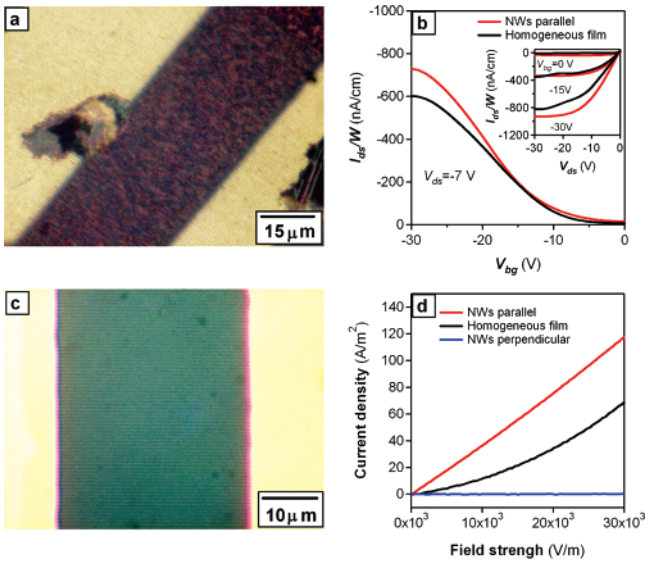

Figure 4. Charge transport properties of PQT and PPy nanowire arrays. (a) POM image of a FET prototype made of PQT nanowires (~320 nm in width). The channel consists of about 90 PQT nanowires perpendicular to the gold source and drain. The electrodes were slightly damaged by the contacting pins during measurement. (b) Width-normalized drain current (I_{ds}/W) vs gate voltage (V_{bg}) at drain-source voltage $V_{ds} = -7$ V for the nanowire-based FET (red) and a FET based on an identically processed homogeneous PQT film (black). The inset shows the normalized drain current (I_{ds}/W) vs V_{ds} at various V_{bg}. The mobility of this specific nanowire FET is larger by a factor of 1.6 compared to the FET based on the homogeneous film processed in a strictly identical fashion. (c) POM image of an array of PPy nanowires contacted for conductivity measurements. (d) Current density vs field strength for PPy nanowires (measured in the perpendicular and parallel directions) and for an identically processed homogeneous PPy film. The parallel conductivity of the nanowire array is larger by a factor of 1.7 compared to the one of the homogeneous PPy film.

hysteresis) according to $I_{ds} = \mu_{lin} \cdot C_i \cdot W/L \cdot (V_{bg} - V_{th}) \cdot V_{ds}$, where $C_i = 33$ nF/cm^2 is the gate dielectric capacitance, V_{th} is the threshold voltage, and W is the active width of the device, that is, the width W^{el} of the electrodes for the homogeneous film, or the product between nanowire width and number of probed nanowires. The mobility in the embossed regions was found to be consistently larger by a factor of 1.7 ± 0.1 compared to the mobility found in homogeneous regions of the same film (average value obtained from 10 different measurements on 5 different samples with a standard deviation of 0.35) with the mobility being typically in the 10^{-5}~10^{-4} cm^2/V·s range depending on details of the processing. These values are somewhat below previously published values,[28] suggesting that further improvement of the carrier mobility is possible by proper modification of the gate dielectric surface as well as control of electrodes' design and exposure to fabrication environment. Nevertheless, the relative increase of the mobility in the nanowires is close to the theoretical factor of 2 expected upon passing from an isotropic to a uniaxial bidimensional material, again confirming the improved orientation of the chains in the nanowires. Devices fabricated with electrodes aligned parallel to the PQT nanowires revealed no electrical conduction.

The electrical conductivity at room temperature of 275 nm wide PPy nanowires was also evaluated in the device shown in Figure 4c, using Au electrodes. In the direction perpendicular to the nanowires, we could not detect any current flow within the experimental accuracy of the method, further indicating the complete isolation of the PPy nanowires. Along the nanowires, the current−voltage ($I-V$) characteristic is ohmic. The resistivity was obtained from the $(dI/dV)^{-1}$ values at zero bias. The resistivity is 259 Ω·m, 1.7 times lower than the one found for the similarly processed isotropic film. Because the nanowire arrays have a higher surface-to-volume ratio than PPy films, PPy nanowires are expected to be more sensitive to extrinsic effects and, hence, display a higher resistivity. This is not the case because of the increased internal orientation of the chains in the nanowires, which is confirmed by the factor of about 2 decrease in resistivity.

Summing up, we have demonstrated that the residue-free embossing of liquid crystalline and amorphous conjugated polymers provides a new simple but versatile approach to the massive fabrication of arrays of organic nanowires of highly controlled internal degree of order. This improved degree of order translates into desirable properties, such as higher conductivity and carrier mobility, or polarized luminescence. Other properties such as mechanical properties are expected to be improved as well, although this was not the purpose of the present paper. Considering the extreme simplicity of the process, the large range of substrates compatible with it, and the benefits brought by the improved degree of internal order, we expect the method to find widespread use for the fabrication of cheap plastic-based nanodevices, including not only those suggested by the systems reported here but also others such as feedback lasers, photodetectors, light-emitting diodes, and high-sensitivity sensors.

Acknowledgment. The authors thank A. Vlad for metallization and the DICE clean room team for providing access to experimental facilities. S.D.C., B.N., and S.M. are Research Associates of the F.R.S.-FNRS. Financial support was provided by the Fondation Louvain (Fonds de Recherche Solvay), the Wallonia Region (NANOSENS, ETIQUEL, and NANOTIC contracts), the FRIA (B.M., L.G.), the Communauté Française de Belgique (ARC NANOMOL), and the Belgian Federal Science Policy (IAP-PAI P6/27).

Supporting Information Available: Materials, nanostructure fabrication, structural characterization of nanowires and of uniform thin films, and opto-electrical measurements. This material is available free of charge via the Internet at http://pubs.acs.org.

References

(1) Cui, Y.; Wei, Q.; Park, H.; Lieber, C. M. *Science* **2001**, *293*, 1289.
(2) Huang, M. H.; Mao, S.; Feick, H.; Yan, H.; Wu, Y.; Kind, H.; Weber, E.; Russo, R.; Yang, P. *Science* **2001**, *292*, 1897.
(3) Duan, X.; Huang, Y.; Agarwal, R.; Lieber, C. M. *Nature* **2003**, *421*, 241.
(4) Zhong, Z.; Wang, D.; Cui, Y.; Bockrath, M. W.; Lieber, C. M. *Science* **2003**, *302*, 1377.

(5) Forrest, S. R. *Nature* **2004**, *428*, 911.
(6) Nguyen, T.-Q.; Wu, J.; Doan, V.; Schwartz, B. J.; Tolbert, S. H. *Science* **2000**, *288*, 652.
(7) Sirringhaus, H.; Brown, P. J.; Friend, R. H.; Nielsen, M. M.; Bechgaard, K.; Langeveld-Voss, B. M. W.; Spiering, A. J. H.; Janssen, R. A. J.; Meijer, E. W.; Herwig, P.; de Leeuw, D. M. *Nature* **1999**, *401*, 685.
(8) Kubo, Y.; Kitada, Y.; Wakabayashi, R.; Kishida, T.; Ayabe, M.; Kaneko, K.; Takeuchi, M.; Shinkai, S. *Angew. Chem., Int. Ed.* **2006**, *45*, 1548.
(9) Dyreklev, P.; Berggren, M.; Inganas, O.; Anderson, M. R.; Wennestrom, O.; Hjertberg, T. *Adv. Mater.* **1995**, *7*, 43.
(10) Montali, A.; Bastiaansen, C.; Smith, P.; Weder, C. *Nature* **1998**, *392*, 261.
(11) Derue, G.; Coppee, S.; Gabriele, S.; Surin, M.; Geskin, V.; Monteverde, F.; Leclere, P.; Lazzaroni, R.; Damman, P. *J. Am. Chem. Soc.* **2005**, *127*, 8018.
(12) Kim, J.; Swager, T. M. *Nature* **2001**, *411*, 1030.
(13) Yu, G.; Cao, A.; Lieber, C. M. *Nature Nanotech.* **2007**, *2*, 372.
(14) Zhang, F.; Nyberg, T.; Inganäs, O. *Nano Lett.* **2002**, *2*, 1373.
(15) Donthu, S.; Pan, Z.; Myers, B.; Shekhawat, G.; Wu, N.; Dravid, V. *Nano Lett.* **2005**, *5*, 1710.
(16) Park, S.; Lim, J.-H.; Chung, S.-W.; Mirkin, C. A. *Science* **2004**, *303*, 348.
(17) O'Brien, G. A.; Quinn, A. J.; Tanner, D. A.; Redmond, G. *Adv. Mater.* **2006**, *18*, 2379.
(18) Jager, E. W. H.; Smela, E.; Inganäs, O. *Science* **2000**, *290*, 1540.
(19) Chou, S. Y.; Krauss, P. R.; Renstrom, P. J. *Science* **1996**, *272*, 85.
(20) Voicu, N. E.; Ludwigs, S.; Crossland, E. J. W.; Andrew, P.; Steiner, U. *Adv. Mater.* **2007**, *19*, 757.
(21) Suh, K. Y.; Lee, H. H. *Adv. Funct. Mater.* **2002**, *12*, 405.
(22) Mele, E.; Di Benedetto, F.; Persano, L.; Cingolani, R.; Pisignano, D. *Nano Lett.* **2005**, *5*, 1915.
(23) Zheng, Z.; Yim, K.-H.; Saifullah, M. S. M.; Welland, M. E.; Friend, R. H.; Kim, J.-S.; Huck, W. T. S. *Nano Lett.* **2007**, *7*, 987.
(24) Stutzmann, N.; Tervoort, T. A.; Bastiaansen, K.; Smith, P. *Nature* **2000**, *407*, 613.
(25) Stutzmann, N.; Friend, R. H.; Sirringhaus, H. *Science* **2003**, *299*, 1881.
(26) Chen, S. H.; Su, A. C.; Su, C. H.; Chen, S. A. *Macromolecules* **2005**, *38*, 379.
(27) Zhao, N.; Botton, G. A.; Zhu, S.; Duft, A.; Ong, B. S.; Wu, Y.; Liu, P. *Macromolecules* **2004**, *37*, 8307.
(28) Ong, B. S.; Wu, Y.; Liu, P.; Gardner, S. *J. Am. Chem. Soc.* **2004**, *126*, 3378.
(29) Hu, Z.; Baralia, G.; Bayot, V.; Gohy, J.-F.; Jonas, A. M. *Nano Lett.* **2005**, *5*, 1738.
(30) Lalanne, P.; Hugonin, J.-P. *J. Opt. Soc. Am. A* **1998**, *15*, 1843.

NL071869J